Title

Diabetes With Multiple Autoimmune and Inflammatory Conditions Linked to an Activating SKAP2 Mutation.

Journal

Diabetes Care, 44(8)

ISSN

1066-9442

Authors

Rutsch, Niklas
Chamberlain, Chester E
Dixon, Wesley
et al.

Publication Date

2021-08-01

DOI

10.2337/dc20-2317

Peer reviewed

Diabetes With Multiple Autoimmune and Inflammatory Conditions Linked to an Activating SKAP2 Mutation

Diabetes Care 2021;44:1816–1825 | https://doi.org/10.2337/dc20-2317

Niklas Rutsch,[1,2,3] Chester E. Chamberlain,[4,5,6] Wesley Dixon,[1,2] Lauren Spector,[1,2] Lisa R. Letourneau-Freiberg,[7] Wint W. Lwin,[4,5] Louis H. Philipson,[7] Alexander Zarbock,[3] Karline Saintus,[4,5,6] Juehu Wang,[4,5,6] Michael S. German,[4,5,6] Mark S. Anderson,[4,5] and Clifford A. Lowell[1,2]

OBJECTIVE

Multiple genome-wide association studies have identified a strong genetic linkage between the *SKAP2* locus and type 1 diabetes (T1D), but how this leads to disease remains obscure. Here, we characterized the functional consequence of a novel *SKAP2* coding mutation in a patient with T1D to gain further insight into how this impacts immune tolerance.

RESEARCH DESIGN AND METHODS

We identified a 24-year-old individual with T1D and other autoimmune and inflammatory conditions. The proband and first-degree relatives were recruited for whole-exome sequencing. Functional studies of the protein variant were performed using a cell line and primary myeloid immune cells collected from family members.

RESULTS

Sequencing identified a de novo *SKAP2* variant (c.457G>A, p.Gly153Arg) in the proband. Assays using monocyte-derived macrophages from the individual revealed enhanced activity of integrin pathways and a migratory phenotype in the absence of chemokine stimulation, consistent with SKAP2 p.Gly153Arg being constitutively active. The p.Gly153Arg variant, located in the well-conserved lipid-binding loop, induced similar phenotypes when expressed in a human macrophage cell line. SKAP2 p.Gly153Arg is a gain-of-function, pathogenic mutation that disrupts myeloid immune cell function, likely resulting in a break in immune tolerance and T1D.

CONCLUSIONS

SKAP2 plays a key role in myeloid cell activation and migration. This particular mutation in a patient with T1D and multiple autoimmune conditions implicates a role for activating *SKAP2* variants in autoimmune T1D.

Recent insights into type 1 diabetes (T1D) have come from genome-wide association studies (GWAS) and studies of rare monogenic disorders that have implicated a host of genes involving immune cell function (1–12). Multiple GWAS have identified a strong genetic linkage between the Src kinase-associated phosphoprotein 2 (*SKAP2*) locus and T1D (6,13,14). SKAP2 is a signaling adaptor protein that plays a key role in mediating integrin responses in monocyte-derived cell populations like macrophages (15,16), but linking how common noncoding risk variants near SKAP2

[1]Department of Laboratory Medicine, University of California San Francisco, San Francisco, CA
[2]The Program in Immunology, University of California San Francisco, San Francisco, CA
[3]Department of Anesthesiology, Intensive Care, and Pain Medicine, University Hospital Münster, University of Münster, Münster, Germany
[4]Diabetes Center, University of California San Francisco, San Francisco, CA
[5]Department of Medicine, University of California San Francisco, San Francisco, CA
[6]Eli and Edythe Broad Center of Regeneration Medicine and Stem Cell Research, University of California San Francisco, San Francisco, CA
[7]Section of Adult and Pediatric Endocrinology, Diabetes, and Metabolism and the Kovler Diabetes Center, The University of Chicago, Chicago, IL

Corresponding authors: Michael S. German, michael.german@ucsf.edu, Mark S. Anderson, mark.anderson@ucsf.edu, and Clifford A. Lowell, clifford.lowell@ucsf.edu

Received 17 September 2020 and accepted 9 March 2021

This article contains supplementary material online at https://doi.org/10.2337/figshare.14192315.

N.R., C.E.C., and W.D. are co-first authors.

alter its activity has remained obscure. Rapid advances in next-generation sequencing have now allowed for a deeper exploration and discovery of rare variants that are linked to disease with techniques like whole-exome sequencing (WES) (17). Here, we used a similar approach to identify a de novo *SKAP2* variant (p.Gly153Arg) in a single patient with T1D and other autoimmune and inflammatory features, and we leveraged this finding to identify a functional alteration in SKAP2. Monocyte-derived macrophages from the individual displayed enhanced activity of integrin pathways and a migratory phenotype in the absence of chemokine stimulation, consistent with SKAP2 p.Gly153Arg being constitutively active. The p.Gly153Arg variant, located in the well-conserved lipid-binding loop, induced similar phenotypes when expressed in a human macrophage cell line. When combined with previous GWAS, our findings suggest that activating *SKAP2* variants result in T1D with comorbid autoimmune and inflammatory disease by promoting increased activity and migration of macrophages.

RESEARCH DESIGN AND METHODS

Study Approval

This study was approved by the institutional review boards at the University of California, San Francisco (UCSF), and The University of Chicago. The proband and her family members were consented for participation through The University of Chicago Monogenic Diabetes Registry (https://monogenicdiabetes.uchicago.edu/registry), which collects longitudinal information regarding diagnosis and treatment of diabetes, other medical problems or complications, family history of diabetes, and results of genetic testing through surveys and medical records.

WES and Analysis

Genomic DNA extraction, targeted capture, and massive parallel sequencing were performed using standard procedures. Briefly, genomic DNA was sheared by Covaris S2 (Covaris Inc., Woburn, MA) to a target size of 200–300 base pairs and assembled into a library with TruSeq adapters containing indexes that differentiate libraries in a capture reaction as well as a sequencing run (Kapa Biosystems, Wilmington, MA). Libraries were pooled into a capture reaction that contains biotinylated DNA oligonucleotides (called "baits") from SeqCap EZ Human Exome Library v3.0 (Roche-Nimblegen, Madison, WI) for 72 h. The DNA–bait-DNA hybrids were then pulled out of the complex mixture by incubation with streptavidin-labeled magnetic beads and captured onto a strong magnet. After washing, the targeted DNA of interest was eluted and subjected to 18 cycles of DNA amplification. Captured DNA libraries were sequenced with the HiSeq 2500 System (Illumina, Hayward, CA), yielding 150 (2 $\times$ 75) base pairs from the final library fragments. Sequence data were mapped to the GRCh37 reference genome and analyzed using the Ingenuity Variant Analysis platform (QIAGEN, Venlo, the Netherlands). Variants identified by WES were filtered using criteria in Supplementary Fig. 6. Sanger sequencing of SKAP2 variant was performed using standard methods with the following primers: forward: ATTGGCTATGATAATTGGGAG; reverse: CTGGTATTTGGAGCATTTGTC.

Culture and Differentiation of THP-1 Monocytes

THP-1 cells (TIB-202; ATCC) were cultured in RPMI medium with 1$\times$ L-glutamine (Corning), 10% heat-inactivated FBS (Gibco), and 1$\times$ penicillin/streptomycin (Gibco). Cells were maintained at a density between 0.2 and 1 $\times$ 10^6 cells/mL. To differentiate the cells into a macrophage-like cell for experimentation, THP-1 cells were added to fresh culture media containing 10 ng/mL phorbol 12-myristate 13-acetate (#534400; Calbiochem) and plated at a density of 1 $\times$ 10^6 cells/mL on nontissue culture–treated dishes. The differentiation media was removed after 72 h, and the adherent cells were rested in normal culture media for 24 h before experimentation. If the cells were to be used for analysis of phosphorylation status, the media in the wells was changed to culture media with 2% heat-inactivated FBS to reduce background kinase signaling. If used for immunofluorescence microscopy, cells were differentiated at a density of 10^5 cells/well in eight-well–chambered slides (#154534; LabTek).

Generation of SKAP2-Null THP-1 Monocytes Using CRISPR-Cas9

Generation of SKAP2-null THP-1 monocytes using CRISPR-Cas9 was performed by following the protocol outlined by Hultquist et al. (18) using the Amaxa 4D-Nucleofector system (#AAF-1002X; Lonza). Guide RNAs were assembled by mixing trans-activating crispr RNA (crRNA) (#1072533; Integrated DNA Technologies) with predesigned crRNA (design identifier Hs.Cas9.SKAP2.1.AD; Integrated DNA Technologies) and incubating for 30 min at 37°C. Purified Cas9 endonuclease (Berkeley QB3 MacroLab) was added to the guide RNA and incubated for 15 min at 37°C. Five hundred thousand undifferentiated THP-1 cells suspended in Amaxa nucleoporation solution (#V4XC-3024; Lonza) were added to 96-well Nucleocuvette Plates and nucleofected using the Amaxa 4D-Nucleofector X Unit 96-well Shuttle system with the program FF-100. Nucleofected cells were rested for 4 days in 96-well plates in RPMI medium with 1$\times$ L-glutamine (Corning), 10% heat-inactivated FBS (Gibco), and 1$\times$ penicillin/streptomycin (Gibco). After resting, the edited cells were counted and seeded at one cell per well, and clones were expanded. Clones were assessed for biallelic SKAP2 editing by DNA sequencing around the expected editing site followed by Tracking of Indels by Decomposition (TIDE) analysis using the TIDE webtool (https://tide.nki.nl). Western blot analysis with an antibody against Skap2 (#12926-1-AP; Proteintech) was also used to confirm the loss the protein expression. Cell lines that developed insertions and deletions causing premature stop codons on both alleles of SKAP2 and that showed no expression of the Skap2 protein were considered Skap2-null. Sequences used were as follows: SKAP2 crRNA (Hs.Cas9.SKAP2.1.AD), 5′-CCTCTCTCATCATAATCCTC-3′; SKAP2 TIDE PCR forward primer, 5′-AGATGCTGAAGAATGGGTACAG-3′; and SKAP2 TIDE PCR reverse primer, 5′-GCCACAAGTCCCA AGAGATTA-3′.

Retroviral Transduction of THP-1 Cells

The wild-type and mutant SKAP2 genes were cloned into the multiple cloning sites of pMIG-W transfer plasmids using standard restriction cloning methods. Amphotropic retroviruses were then produced using third-generation methods by the UCSF ViraCore (https://viracore.ucsf.edu). SKAP2-null THP-1 cells were transduced by resuspending 1 $\times$ 10^6 cells in 1 mL of the retroviral

supernatant supplemented with 8 μg/mL protamine sulfate (#20FK79; W.W. Grainger, Inc.) and centrifuging the suspension in a tissue culture–treated six-well plate at 2,000 rpm for 1 h at room temperature (RT). Following centrifugation, an additional 1 mL of culture media was added to each well, and the cells rested for 1 day in a 37°C incubator. After 1 day, the cell media containing the retroviral supernatant were removed, and the cells were resuspended in 3 mL culture media. The cells were sorted on a FACSAria machine on the basis of GFP expression 3 days following transduction. Western blot analysis using a Skap2 antibody (#12926-1-AP; Proteintech) was performed to confirm the expression of the transduced *SKAP2* gene.

Western Blotting and Integrin Stimulation

Wells of nontissue culture–treated six-well plates (#CLS3736; Corning) were coated for 1 h at RT with 1 mL of 2 μg/mL fibronectin-like engineered peptide (#F8141; Sigma) in Hanks' balanced salt solution (HBSS) with 20 mmol/L HEPES or 5% nonfat dry milk (Bio-Rad) in HBSS with 20 mmol/L HEPES. Wells were washed once with deionized water before seeding cells. THP-1 cells or primary monocytes derived from the patient were gently detached from their culture wells using 5 mmol/L warm EDTA in Dulbecco's PBS. Cells were then seeded into the coated wells at a density of 1.2 $\times$ 10^6 cells/well. The plates were centrifuged at 500 rpm at 4°C for 3 min to allow for simultaneous integrin activation and then incubated for 45 min at 37°C. Both adherent and suspended cells were then lysed in the wells using 200 μL ice-cold radioimmunoprecipitation assay buffer for 10 min and centrifuged at 13,000 rpm for 10 min at 4°C. The supernatant was transferred to cold 1$\times$ NuPage LDS Sample Buffer (Invitrogen) containing 1$\times$ NuPage Sample Reducing Agent (Invitrogen). Samples were loaded in a 4–12% gradient NuPage (Invitrogen) gel and blotted using semidry transfer onto a polyvinylidene fluoride membrane. Membranes were blocked with 5% nonfat dry milk or 5% BSA (Sigma) in Tris-buffered saline with Tween (TBS-T) and were stained and incubated with primary antibodies (see Supplementary Table 4) in 5% BSA and TBS-T at 4°C overnight. After washing with TBS-T, the secondary IR-Dye antibodies (see Supplementary Table 5) were added to the membrane and incubated for 30 min at RT in TBS-T containing 5% BSA and 0.1% SDS. The membrane was imaged and quantified with the LI-COR Odyssey CLx and Image Studio (LI-COR) software. Antibodies are listed in Supplementary Tables 4 and 5.

Isolation of Primary Human Monocytes Through Density Gradient Centrifugation

Blood was collected in 10-mL heparinized tubes and brought to RT. In equal amounts, Histopaque 1077 (Sigma) was layered on top of Histopaque 1119 (Sigma) in a sterile 15-mL reaction tube (Falcon). The final layer was an equal amount of blood. The tube was centrifuged at 900*g* for 30 min at RT, using the lowest settings on brake and acceleration. The isolation yields three major layers which, from top to bottom, are the thrombocyte/monocyte/T-cell layer, the neutrophil granulocytes, and the erythrocyte pellet. The top layer was collected and washed in 20 mmol/L HEPES-buffered HBSS. Residual erythrocytes were then lysed for 90 s in 5.25 mL distilled water and 1.25 mL HBSS/20 mmol/L HEPES, after which isotonicity was restored by addition of 2.2 mL of 3% NaCl before centrifugation. Cells were resuspended in HBSS/20 mmol/L HEPES and counted. The top layer monocytes were resuspended in 1 mL heat-inactivated FBS (Gibco) containing 10% DMSO (Sigma) and stored in liquid nitrogen until further use.

Culture of Primary Human Monocyte-Derived Macrophages

Monocytes were cultured using RPMI medium with 1$\times$ L-glutamine (Corning), 10% heat-inactivated FBS (Gibco), 1$\times$ penicillin/streptomycin (Gibco), and 50 ng/mL human recombinant granulocyte-monocyte colony-stimulating factor (215-GM-010; R&D Systems). The whole supernatant was discarded and replenished with fresh media after 3 days. Experiments and staining were performed following day 7 of the differentiation period. For immunofluorescence microscopy, monocytes were cultured at a density of 10^5 cells/well in eight-well–chambered slides (#154534; LabTek). For Western blotting, cells were differentiated in 6-cm culture dishes (Corning).

Single-Cell RNA Sequencing of Patient Neutrophils

Blood samples from the SKAP2 patient and control subject were collected in heparinated tubes. Then, red blood cells were lysed (BD Pharm Lyse lysing buffer, Cat #555899; BD Biosciences), and samples were washed with sterile FACS buffer (HBSS [Gibco], 2 mmol/L EDTA, and 2% heat-inactivated FBS [Gibco]). After blocking for 5 min (Human BD Fc Block, Cat #555899; BD Pharmigen), specimens were stained with aqua dye (#L34957, 1:100; Invitrogen) and anti-CD45 (Cat #555485, RRID:AB_398600, 1:20; BD Biosciences) for 20 min at 37°C and 5% CO_2 in a humidified incubator. Finally, samples were washed again and filtrated into sterile flow cytometry tubes (#352058; Corning). One hundred fifty thousand cells were sorted using a BD Fusion SORP with a 70-μm nozzle in a biosafety cabinet. Fifty thousand cells were transferred to 0.04% BSA (Sigma) in DPBS (Gibco) also containing 1 unit/μL RNAse inhibitor (PN-3335399001; Sigma-Aldrich). Sample processing was performed using Chromium Technology (10$\times$ Genomics) to the manufacturer's instructions with 5′-primed and T-cell receptor sequencing. Sample barcoding and demultiplexing and single-cell counting were performed using the 10$\times$ Genomics Cell Ranger Single Cell Software Suite. The reads were aligned to GRCh38 (the 3.0.0 version from the Cell Ranger website) with Cell Ranger 3.0.2 using the Cell Ranger count command with the default settings. Reads were quantified and filtered using Cell Ranger count. The Seurat package (19) in R was used for the following downstream analysis (https://www.rstudio.com). First, cells with mitochondrial gene expression $>$7.5%, RNA count $<$200 and $>$25,000, and feature RNA $<$100 and $>$2,500 were excluded. Samples were then scaled with factor 10,000, and the two samples (SKAP2 p.Gly153Arg patient and SKAP2 wild-type control) were integrated with the 2,000 most variable features. Principal component analysis was performed next, and dimensionality for clustering was determined using an elbow plot. Uniform manifold approximation

and projection clustering was performed on the first 21 principal components. To identify the marker genes for each cluster, the differential gene expression of that cluster was compared with all the other clusters. Using the packages EnhancedVolcano (https://github.com/kevinblighe/EnhancedVolcano) and Pathview (20) in the Bioconductor Project Package Repository (https://CRAN.R-project.org/package=BiocManager) in R, further integrated downstream analysis was performed, testing the SKAP2 G153R sample against the SKAP2 wild-type control sample. Pathway analysis was based on the "org.HS.eg.db" pathway gene library with a *P* value cutoff of 0.05.

Immunofluorescence Microscopy

For stimulation assays, monocyte-derived macrophages and THP-1 cells were stimulated with monocyte differentiation media or THP-1 culture media containing either 100 ng/mL C-C motif chemokine 2 (CCL2) (#Z02829; GenScript) or 100 ng/mL recombinant human C-X-C motif chemokine ligand 1 (CXCL1) (#275-GR-010; R&D Systems) and were stained directly in their wells. Cells were fixed in 4% paraformaldehyde (Sigma) in DPBS (Gibco) containing 2 mmol/L $MgCl_2$ and 1 mmol/L $CaCl_2$ ($PBS^{+/+}$) for 15 min at RT. After washing with $PBS^{+/+}$, cells were permeabilized with 0.1% Triton X-100 in $PBS^{+/+}$ for 10 min at RT. Followed by another wash, cells were blocked with 5% BSA in $PBS^{+/+}$ for 1 h at RT and then stained with primary antibodies against SKAP2 (Cat #12926-1-AP, RRID:AB_2189317, 1:200; Proteintech) and Wiskott-Aldrich syndrome protein (WASp) (sc-5300, RRID:AB_628446, 1:50; Santa Cruz Biotechnology) in 1% BSA/$PBS^{+/+}$ and incubated overnight at 4°C. Secondary staining was then performed with Alexa Fluor 488 donkey anti-rabbit IgG (H&L) (A-21206, RRID:AB_2535792, 1:1,000; Thermo Fisher Scientific), Alexa Fluor 647 goat anti-mouse IgG (H&L) (ab150115, RRID:AB_2687948, 1:1,000; Abcam), and Alexa Fluor 546 Phalloidin (A-22283, RRID:AB_2632953, 1:40; Thermo Fisher Scientific) in 1% BSA in $PBS^{+/+}$ for 1 h at RT. Slides were mounted using ProLong Gold Antifade Mountant with DAPI (P36934; Thermo Fisher Scientific) and sealed with nail polish (#72180; Electron Microscopy Science).

Immunofluorescence microscopy of fixed and phalloidin-stained cells was performed using a Zeiss Axio Imager M2 with Apotome 2 configuration using ZEN Blue Pro software (Zeiss). Confocal microscopy was performed with the Nikon A1R using NIS Elements software, and Imaris 9.5 (Oxford Instruments) was used for image processing. Colocalization analysis was done using confocal images of fixed cells stained for SKAP2 and WASp proteins and then for calculating the ratio of positive cells to total cells per condition. Scoring of positive cells was performed using three blinded, independent scorers. Cell shape analysis was performed using ImageJ and an ImageJ macro (Supplementary Fig. 7).

Statistics

For quantification of colocalization and shape change analyses, data sets were compared by two-way ANOVA, and *P* values were adjusted with Tukey multiple comparisons test using R Studio software (https://www.RStudio.com). pERK/ERK quantification data were compared by Student *t* test using Excel software (Microsoft Corporation). Quantification of colocalization and pERK/ERK data is displayed as mean ± SE. Quantification of shape change data is displayed as box blots with centered median.

RESULTS

Clinical Characteristics of the Patient With *SKAP2* Variant

In an effort to identify people with T1D with a strong underlying genetic cause, we examined individuals from The University of Chicago Monogenic Diabetes Registry (https://monogenicdiabetes.uchicago.edu/registry) who had been diagnosed with T1D but did not have one of the known forms of monogenic diabetes (e.g., mutations in the insulin gene). Out of 10 families with T1D from the registry selected for WES, we identified a 24-year-old individual with multiple autoimmune conditions (Supplementary Tables 1 and 2) and no known family history of any of these conditions. She initially presented with symptoms of hypothyroidism at the age of 14 years and was incidentally found to have glucosuria, hyperglycemia, and a hemoglobin A_{1c} of 8.4%. Her BMI at that time was near the 50th percentile for age. Her T1D genetic risk score falls within the 25–50th percentile (21), and she is heterozygous for HLA-DR3. She tested positive for autoantibodies against the pancreatic islet β-cell proteins GAD and islet cell antigen 512 and autoantibodies against thyroid proteins thyroglobulin and thyroid peroxidase. Additional medical history included other forms of autoimmunity, including eczema, intermittent hemolytic anemia, undifferentiated connective tissue disease, and Raynaud syndrome. Subsequent testing detected additional autoantibodies, including antinuclear antibody and antitopoisomerase 1 antibody.

In Silico Identification and Characterization of the SKAP2 p.Gly153Arg Variant

WES on DNA samples from the proband (Fig. 1*A*, member II-1), unaffected brother (II-2), and unaffected parents (I-1 and I-2) revealed a novel de novo germline coding variant in the *SKAP2* gene (c.457G>A, p.Gly153Arg) (Supplementary Table 3) that encodes for SKAP2 protein. Sanger sequencing confirmed that the *SKAP2* variant was present in the affected family member and absent in unaffected family members (Fig. 1*B*). Parenthood was confirmed with rare single nucleotide polymorphisms identified by WES. The variant was not found in >270,000 alleles in the Genome Aggregation Database (22). No *SKAP2* mutations are known to cause human disease, although GWAS have linked single nucleotide polymorphisms in the *SKAP2* locus to autoimmune diseases, including T1D (6,23–25,28).

Species alignment showed that Gly153 is highly conserved in SKAP2 from species as distant as *Xenopus tropicalis* and *Danio rerio* (Fig. 1*C*). SKAP2 forms a homodimer using an N-terminal four-helix bundle dimerization domain (DM), against which its two pleckstrin homology (PH) domains arrange in a conformation incompatible with phosphoinositide binding (Fig. 1*D*). Biochemical, cell biological, and crystallographic studies of SKAP2 have demonstrated that the DM and PH domains form a lipid-responsive molecular switch (26). Lipid binding induces a conformational change in SKAP2, allowing it to bind and activate the WASp/Arp2/3 protein complex, which can then initiate actin polymerization at the cell

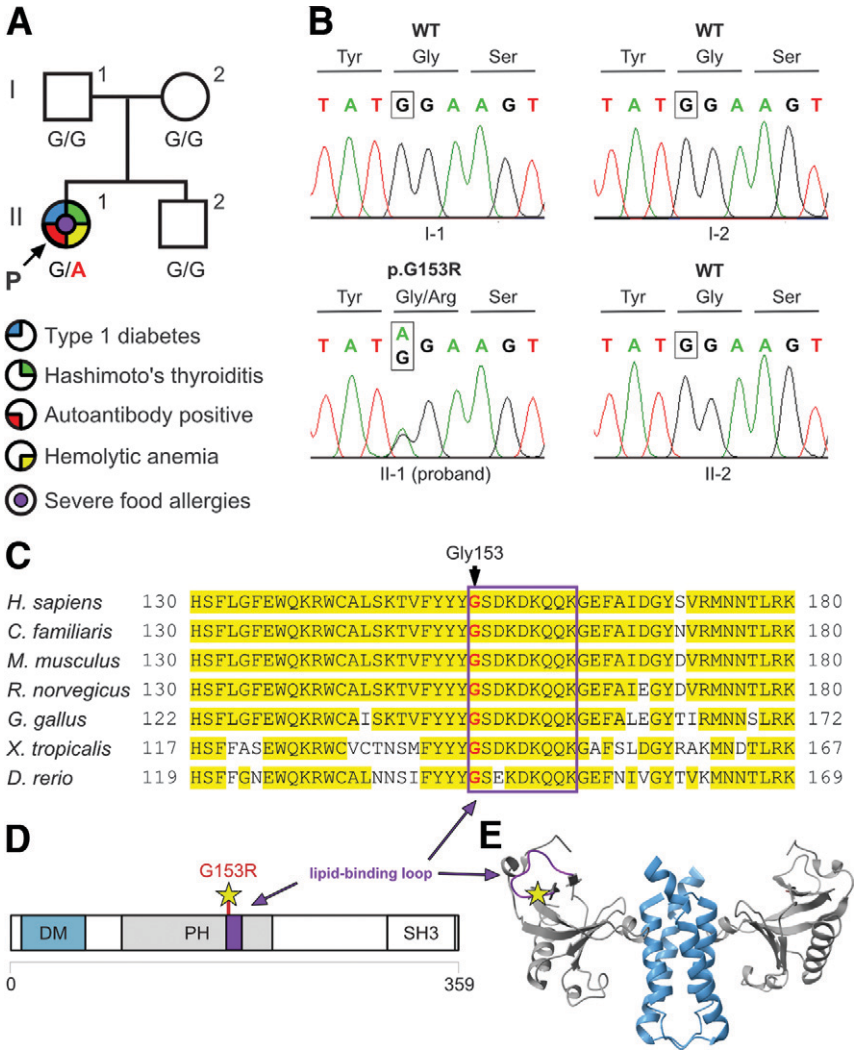

Figure 1—A de novo SKAP2 mutation in the 3′-phosphoinositide binding loop. *A*: Pedigree of kindred. The participant with T1D, Hashimoto thyroiditis, and Raynaud syndrome is shown with a filled symbol, and nonaffected participants are shown with unfilled symbols. *B*: Sanger sequencing chromatograms showing the wild-type (WT) SKAP2 sequence of the unaffected parents (I-1 and I-2) and brother (II-2) and the SKAP2 variant c.457G>A (p.Gly153Arg) identified in the affected proband (II-1). *C*: Alignment and conservation of residues encoded by SKAP2 orthologs. Residues that are conserved in three or more species are highlighted in yellow. p.Gly153Arg is located in a highly conserved lipid-binding loop (box). Several deletions and mutations mapping to this region result in dominant active or negative SKAP2 activity (26). *D*: Schematic of the SKAP2 protein. *E*: Homodimeric 3D structure of the murine SKAP2 DM and PH domains (Protein Data Bank identifier: 2OTX) visualized with ChimeraX (27).

membrane (15,16). Several deletions and mutations mapping to this region result in dominant active or negative SKAP2 activity (26). The p.Gly153Arg variant is located within the highly conserved lipid-binding loop (Fig. 1*E*), suggesting a possible functional consequence.

In Vitro Functional Assessment of the SKAP2 p.Gly153Arg Variant

Genetic studies in mice have shown that SKAP2 is a critical mediator of the "inside-out" and "outside-in" integrin intracellular signaling pathways that regulate cytoskeletal changes in myeloid immune cells (15,16,29). Consistent with these studies, SKAP2 is expressed in immune tissues and is enriched in myeloid cell types (Supplementary Fig. 1). To evaluate the p.Gly153Arg variant, we generated SKAP2-deficient ($SKAP2^{-/-}$) macrophages from the human THP-1 monocyte cell line (30) and reintroduced either wild-type or p.Gly153Arg SKAP2 using retroviral transduction. Western blot analysis of $SKAP2^{-/-}$ THP-1 macrophages confirmed loss of endogenous SKAP2 expression and similar levels of retrovirally expressed wild-type or p.Gly153Arg SKAP2 (Supplementary Fig. 2). $SKAP2^{-/-}$ THP-1 macrophages had reduced integrin-induced phosphorylation of extracellular signal-regulated kinases 1 and 2 (ERK) and did not change shape in response to CCL2 (Supplementary Fig. 2), consistent with the phenotype of murine $Skap2^{-/-}$ macrophages (15).

SKAP2 moves from the cytosol to the cellular membrane in response to chemokine signals, then recruits WASp to drive localized actin polymerization (15,16,31). We therefore assayed for SKAP2 and WASp localization by immunostaining. Both SKAP2 and WASp were detected by immunostaining in the cytoplasm of resting $SKAP2^{-/-}$ THP-1 macrophages infected with lentivirus expressing wild-type SKAP2 (Fig. 2*A*). Nuclear localization of WASp, but not SKAP2, was also observed, consistent with previous reports (32). Treatment with CXCL1, a proinflammatory macrophage chemokine (33), induced significant colocalization of SKAP2 and WASp at the plasma membrane (Supplementary Fig. 3), consistent with the activation of these proteins. In contrast, we found significant colocalization of SKAP2 and WASp at the plasma membrane in resting THP-1 macrophages with lentivirus-expressed SKAP2 p.Gly153Arg (Fig. 2*A* and *B*, arrows), indicating that SKAP2 p.Gly153Arg is active in the absence of chemokine treatment.

SKAP2 also mediates chemokine-stimulated integrin activation, which induces the extracellular region of integrins on the surface of myeloid cells to adopt an open conformation that increases integrin ligand avidity (inside-out signaling). This change increases the cellular response to extracellular integrin ligands (outside-in signaling) (34,35). To assess these integrin pathways, we assayed for the phosphorylation of ERKs following plating of resting THP-1 macrophages on poly-Arg-Gly-Asp (pRGD)–coated surfaces. ERK phosphorylation in resting, untreated cells expressing SKAP2 p.Gly153Arg was significantly higher than in cells expressing wild-type SKAP2 (Fig. 2*C* and *D* and Supplementary Fig. 3), further demonstrating that SKAP2 p.Gly153Arg acts in a dominant active fashion (34,35).

Chemokine activation of actin polymerization and integrin signaling induces shape changes during cellular migration (36). Consistent with this induction, resting

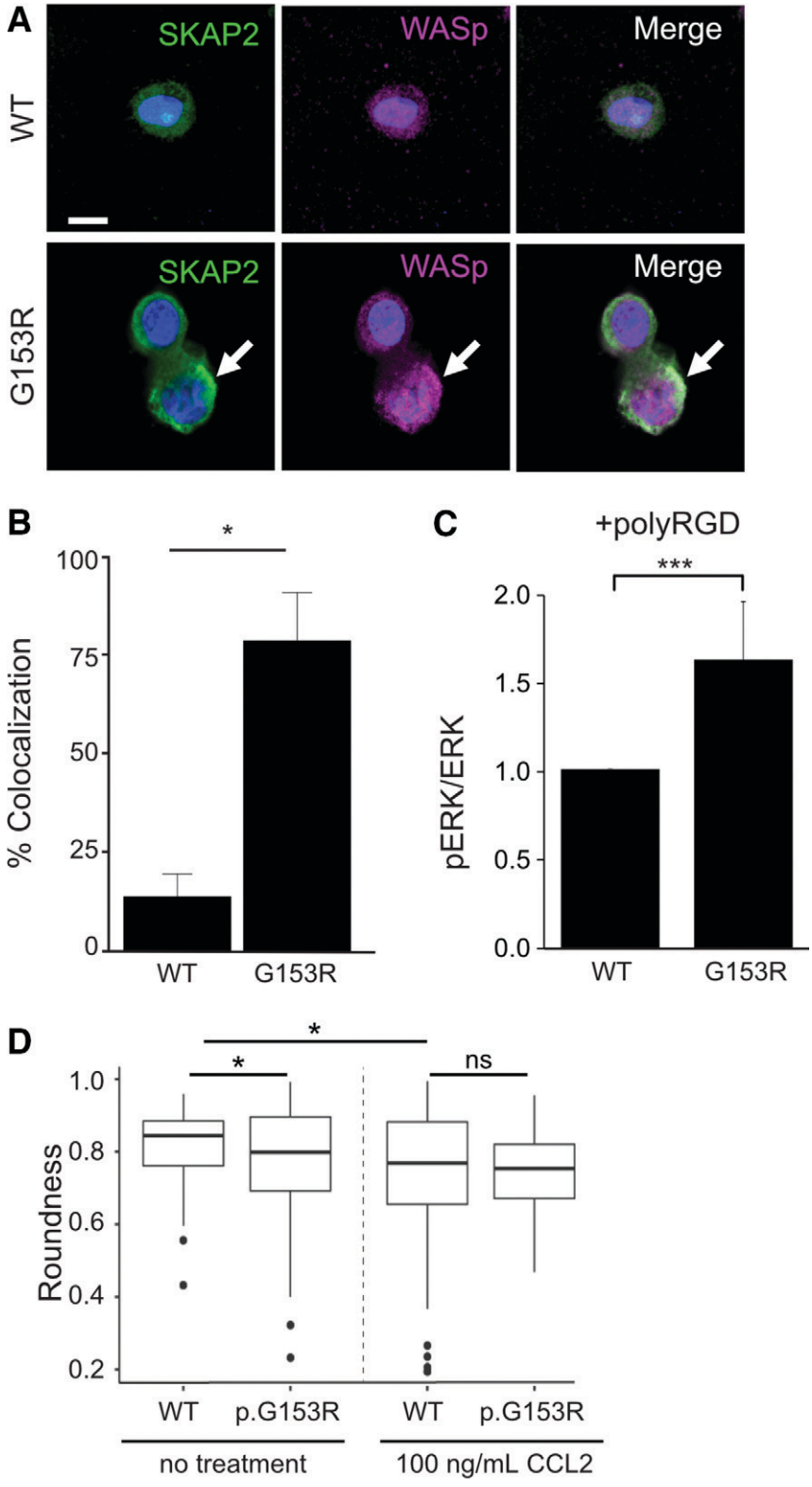

Figure 2—Functional evaluation of the SKAP2 p.Gly153Arg variant in a human macrophage cell line. *A*: Immunostaining for SKAP2 (green) and WASp (purple) in untreated SKAP2$^{-/-}$ THP-1 macrophages expressing either wild-type (WT) or p.Gly153Arg SKAP2 by retroviral transduction. DNA marker DAPI is in blue. Scale bar = 15 µm. *B*: Percent colocalization of SKAP2 and WASp (mean ± SE, two-way ANOVA, $n = 3$). *$P < 0.05$. *C*: Quantification of pERK/ERK in pRGD-plated *SKAP2*$^{-/-}$ THP-1 macrophages expressing either WT or p.Gly153Arg SKAP2 by retroviral transduction (mean ± SE, Student *t* test, $n = 6$). ***$P < 0.001$. *D*: Cell shape analysis of indicated THP-1 macrophages with and without treatment with macrophage chemokine CCL2 (median-centered box plot, two-way ANOVA, $n = 3$). *$P < 0.05$.

THP-1 macrophages expressing wild-type SKAP2 acquired a less rounded, migratory phenotype after treatment with the potent chemokine CCL2 (Fig. 2*E*). In contrast, resting THP-1 macrophages expressing SKAP2 p.Gly153Arg displayed a migratory phenotype in the absence of CCL2 treatment, and their shape did not change further after the addition of CCL2 (Fig. 2*E*).

Next, we evaluated whether primary macrophages carrying the SKAP2 p.Gly153Arg heterozygous allele displayed similar phenotypes by harvesting monocytes from the proband (Fig. 1*A*, II-1, "patient") and unaffected mother (I-2, "control") and then differentiated these cells into macrophages ex vivo. Western blot analysis of patient and control macrophages revealed that the p.Gly153Arg variant did not alter SKAP2 protein expression (Supplementary Fig. 4). In resting control macrophages, wild-type SKAP2 and WASp were largely cytosolic (Fig. 3*A*), while treatment with CXCL1 resulted in significant colocalization of SKAP2 and WASp at the plasma membrane (Supplementary Fig. 5). Strikingly, we found significant colocalization of SKAP2 p.Gly153Arg and WASp at the plasma membrane in resting patient macrophages (Fig. 3*A*, arrows), similar to what was observed in THP-1 macrophages expressing the p.Gly153Arg SKAP2 protein (Fig. 2*A*). Patient macrophages also had higher levels of integrin-activated ERK phosphorylation compared with control cells and assumed a less rounded, more migratory phenotype in the absence of CCL2 treatment (Fig. 3*C* and *D* and Supplementary Fig. 5), similar to observations in THP-1 cells expressing the pGly153Arg SKAP2 variant. Finally, we performed single-cell RNA sequencing on FACS-sorted patient and control neutrophils, another myeloid immune cell population that depends on SKAP2 function (16). Consistent with SKAP2 p.Gly153Arg myeloid cell activation, patient neutrophils showed upregulation of key signaling molecules, including RIPK2, TLR2, IL3RA, and IL1RN, and broad activation of secretory and kinase signaling pathways (Supplementary Fig. 8).

CONCLUSIONS

We identified the first monogenic, functional variant of the *SKAP2* gene linked to

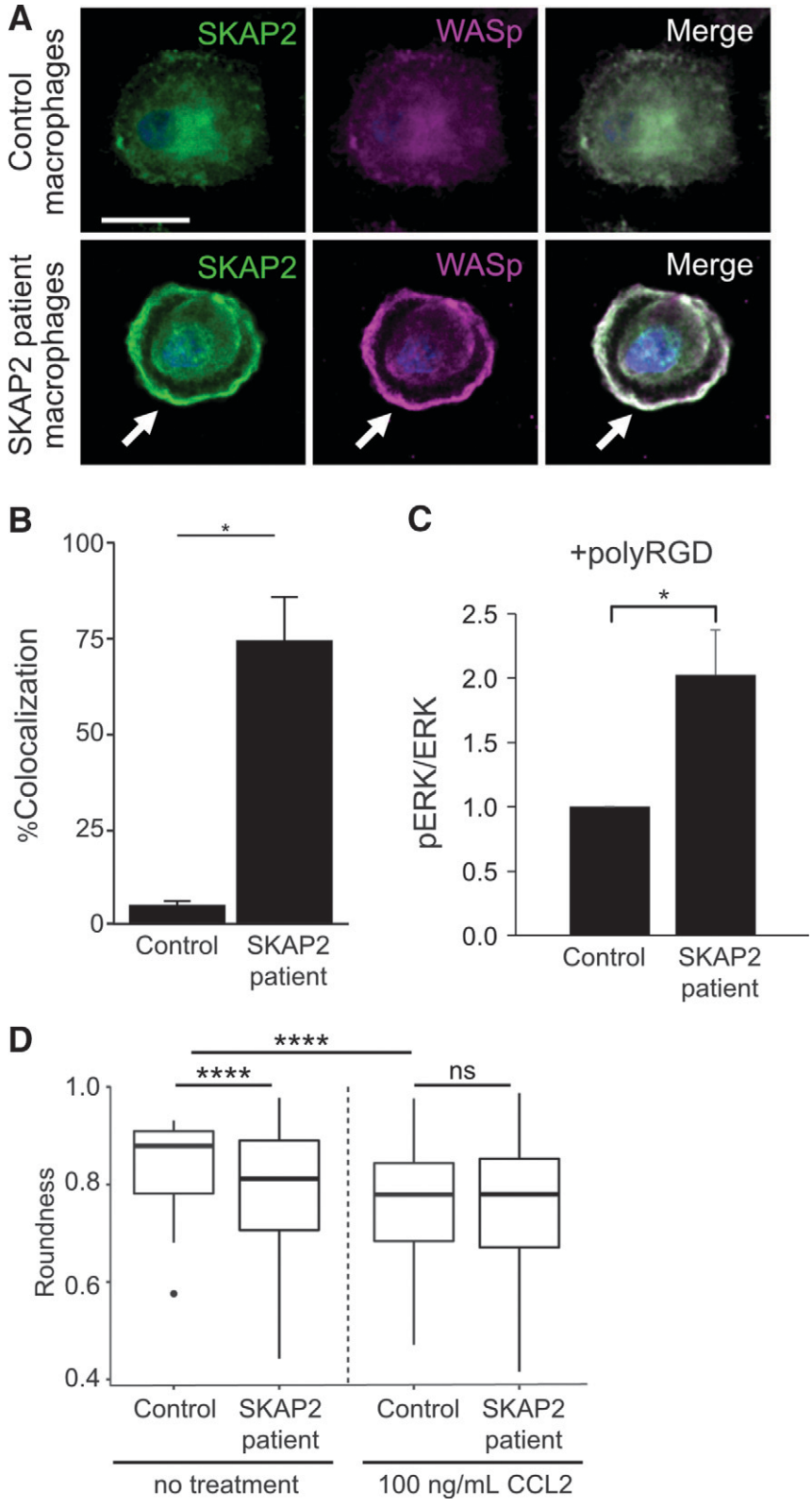

Figure 3—Phenotypes of SKAP2 patient macrophages. *A*: Immunostaining for SKAP2 (green) and WASp (purple) in resting SKAP2 patient and control macrophages. DNA marker DAPI is in blue. Scale bar = 15 µm. *B*: Percent colocalization of SKAP2 and WASp (mean ± SE, two-way ANOVA, $n = 3$). *$P < 0.05$. *C*: Quantification of pERK/ERK in SKAP2 patient and control macrophages plated on pRGD (mean ± SE, Student *t* test, $n = 3$). *$P < 0.05$. *D*: Cell shape analysis of SKAP2 patient and control macrophages with and without treatment with macrophage chemokine CCL2 (median-centered box plot, $n = 3$). ****$P < 0.0001$.

a patient with T1D. Our data show that the SKAP2 p.Gly153Arg protein acts in a dominant active fashion. Because SKAP2 mediates both inside-out and outside-in integrin signaling, we propose that SKAP2 p.Gly153Arg drives the constitutive activation of these pathways in the absence of chemokine signaling, which likely results in the chronic hyperactivity of myeloid immune cell populations that express SKAP2 and contributes to the inflammation underlying autoimmune diabetes and other immune conditions in the patient (Fig. 4).

The development of T1D involves dysregulation of the innate and adaptive arms of the immune system, which is influenced by genetic and environmental factors (37,38). Insights into this dysregulation have come from studies of rare monogenic disorders (12). For example, patients carrying mutations in *AIRE* or *FOXP3* frequently develop T1D, along with other autoimmune disorders. Dissecting the consequences of these mutations has improved our understanding of the role of central T-cell tolerance and T regulatory cells in preventing organ-specific autoimmune diseases like T1D (1,3–12).

SKAP2 is a key regulator of integrin function in myeloid cells of the innate immune system, and numerous studies in humans and mice have observed the persistent activation of these cells during both the initiation and the development of T1D (39–45). In addition, several examples demonstrate that loss-of-function mutations in proteins that act as negative regulators of myeloid cell integrin signaling can lead to autoimmunity (46,47). Loss of these integrin regulators leads to hyperactive myeloid cells, in particular dendritic cells, which drive development of self-reactive T and B cells. In these models, treatments that target integrin signaling components disrupt this circuit and provide some therapeutic benefit (34). Further, hyperactivation of nuclear factor-κB signaling pathways in dendritic cells in mice leads to constitutive inflammatory cytokine production that can also drive autoimmunity (48). Also important to note is that the overactive form of SKAP2 in this patient case is associated with other autoimmune conditions beyond T1D, including thyroiditis and autoimmune hemolytic anemia, revealing a major break in

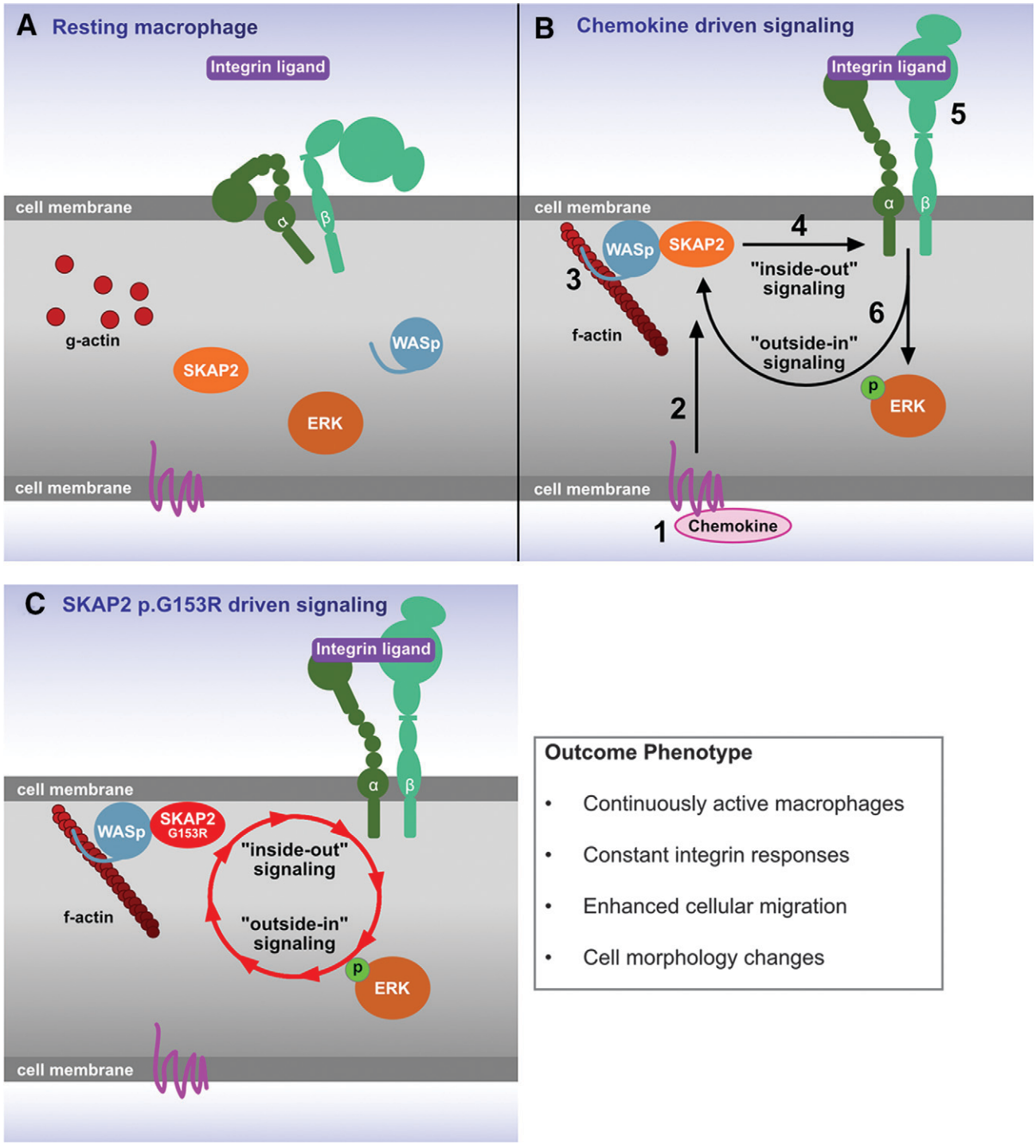

Figure 4—Proposed model for the constitutive activation of macrophages with the SKAP2 p.Gly153Arg mutation. *A*: In the absence of inflammation, macrophages are resting, SKAP2 and WASp are cytosolic, and integrins are in a bent conformation with reduced affinity for extracellular ligands. *B*: In response to inflammatory chemokines (1), SKAP2 is activated (2) and recruits WASp to the cell membrane to initiate actin polymerization (3). Activated SKAP2 also initiates inside-out integrin signaling (4) that results in conformational changes in the extracellular region of the integrins to increase ligand affinity (5). This initiates outside-in integrin signaling (6), which activates multiple intracellular targets such as ERK and SKAP2. *C*: SKAP2 p.Gly153Arg is constitutively active, creating an endless cycle of integrin signaling in the absence of inflammatory chemokines.

immune tolerance in this patient. These findings are consistent with broad overactivity of monocytes and neutrophils, which could promote activation of multiple autoreactive T- and B-lymphocyte populations, resulting in a spectrum of autoimmunity beyond T1D.

Together, our data indicate that mutations in *SKAP2*, which result in gain-of-function constitutive signaling in myeloid lineage cells, can lead to T1D with comorbid autoimmune and inflammatory disease. The precise mechanism for how the inflammation induced by SKAP2 p.Gly153Arg leads to a break in tolerance

and autoimmune diabetes remains to be determined.

Acknowledgments. The authors thank the family for participation in this research study (https://monogenicdiabetes.uchicago.edu). They also thank the following individuals for assistance with sample collection and sample processing: Gail Gannon, Mariko Pusinelli, May Sanyoura, and Balamurugan Kandasamy.

Funding. This work was supported by the Leona M. and Harry B. Helmsley Charitable Trust (G-2018PG-T1D018, G-2003-04376), the Larry L. Hillblom Foundation (2018-D-006-NET), the National Institute of Diabetes and Digestive and Kidney Diseases of the National Institutes of Health (NIH) (R01-DK-104942, P30-DK-020595, T32DK007418), UCSF Parnassus Flow Core RRID:SCR_018206, DRC Center Grant NIH P30 DK-063720, NIH S10 1S10OD021822-01, and a private donor. A.Z. was supported by Deutsche Forschungsgemeinschaft (ZA428/11-1, ZA428/18-1, INST 211/604-1).

Duality of Interest. No potential conflicts of interest relevant to this article were reported.

Author Contributions. N.R., C.E.C., W.D., L.S., and K.S. conducted the experiments and wrote the manuscript. W.W.L. and J.W. helped with WES and analysis. N.R., C.E.C., W.D., L.H.P., A.Z., M.S.G., M.S.A., and C.A.L. designed the study and analyzed the data. N.R., W.D., L.R.L.-F., W.W.L., and L.H.P. helped with human tissue specimens. L.R.L.-F. and L.H.P. recruited the family. C.A.L. is the guarantor of this work and, as such, had full access to all the data in the study and takes responsibility for the integrity of the data and the accuracy of the data analysis.

Prior Presentation. Parts of this study were presented in abstract form at the 81st Scientific Sessions of the American Diabetes Association, Virtual, 25–29 June 2021.

References

1. Dabelea D, Mayer-Davis EJ, Saydah S, et al.; SEARCH for Diabetes in Youth Study. Prevalence of type 1 and type 2 diabetes among children and adolescents from 2001 to 2009. JAMA 2014;311:1778–1786

2. Concannon P, Rich SS, Nepom GT. Genetics of type 1A diabetes. N Engl J Med 2009;360:1646–1654

3. Bottini N, Musumeci L, Alonso A, et al. A functional variant of lymphoid tyrosine phosphatase is associated with type I diabetes. Nat Genet 2004;36:337–338

4. Tang W, Cui D, Jiang L, et al. Association of common polymorphisms in the IL2RA gene with type 1 diabetes: evidence of 32,646 individuals from 10 independent studies. J Cell Mol Med 2015;19:2481–2488

5. Onengut-Gumuscu S, Chen WM, Burren O, et al.; Type 1 Diabetes Genetics Consortium. Fine mapping of type 1 diabetes susceptibility loci and evidence for colocalization of causal variants with lymphoid gene enhancers. Nat Genet 2015;47:381–386

6. Barrett JC, Clayton DG, Concannon P, et al.; Type 1 Diabetes Genetics Consortium. Genome-wide association study and meta-analysis find that over 40 loci affect risk of type 1 diabetes. Nat Genet 2009;41:703–707

7. Cooper JD, Smyth DJ, Smiles AM, et al. Meta-analysis of genome-wide association study data identifies additional type 1 diabetes risk loci. Nat Genet 2008;40:1399–1401

8. Bennett CL, Christie J, Ramsdell F, et al. The immune dysregulation, polyendocrinopathy, enteropathy, X-linked syndrome (IPEX) is caused by mutations of FOXP3. Nat Genet 2001;27:20–21

9. Finnish-German APECED Consortium. An autoimmune disease, APECED, caused by mutations in a novel gene featuring two PHD-type zinc-finger domains. Nat Genet 1997;17:399–403

10. Nagamine K, Peterson P, Scott HS, et al. Positional cloning of the APECED gene. Nat Genet 1997;17:393–398

11. Flanagan SE, Haapaniemi E, Russell MA, et al. Activating germline mutations in STAT3 cause early-onset multi-organ autoimmune disease. Nat Genet 2014;46:812–814

12. Husebye ES, Anderson MS, Kämpe O. Autoimmune polyendocrine syndromes. N Engl J Med 2018;378:1132–1141

13. Lu JM, Chen YC, Ao ZX, et al. System network analysis of genomics and transcriptomics data identified type 1 diabetes-associated pathway and genes. Genes Immun 2019;20:500–508

14. Reddy MV, Wang H, Liu S, et al. Association between type 1 diabetes and GWAS SNPs in the southeast US Caucasian population. Genes Immun 2011;12:208–212

15. Alenghat FJ, Baca QJ, Rubin NT, et al. Macrophages require Skap2 and Sirpα for integrin-stimulated cytoskeletal rearrangement. J Cell Sci 2012;125:5535–5545

16. Boras M, Volmering S, Bokemeyer A, et al. Skap2 is required for β_2 integrin-mediated neutrophil recruitment and functions. J Exp Med 2017;214:851–874

17. Adams DR, Eng CM. Next-generation sequencing to diagnose suspected genetic disorders. N Engl J Med 2018;379:1353–1362

18. Hultquist JF, Hiatt J, Schumann K, et al. CRISPR-Cas9 genome engineering of primary $CD4^+$ T cells for the interrogation of HIV-host factor interactions. Nat Protoc 2019;14:1–27

19. Stuart T, Butler A, Hoffman P, et al. Comprehensive integration of single-cell data. Cell 2019;177:1888–1902.e21

20. Luo W, Brouwer C. Pathview: an R/Bioconductor package for pathway-based data integration and visualization. Bioinformatics 2013;29:1830–1831

21. Oram RA, Patel K, Hill A, et al. A type 1 diabetes genetic risk score can aid discrimination between type 1 and type 2 diabetes in young adults. Diabetes Care 2016;39:337–344

22. Karczewski KJ, Francioli LC, Tiao G, et al. Variation across 141,456 human exomes and genomes reveals the spectrum of loss-of-function intolerance across human protein-coding genes [preprint]. bioRxiv:531210v2

23. Jostins L, Ripke S, Weersma RK, et al.; International IBD Genetics Consortium (IIBDGC). Host-microbe interactions have shaped the genetic architecture of inflammatory bowel disease. Nature 2012;491:119–124

24. Liu JZ, van Sommeren S, Huang H, et al.; International Multiple Sclerosis Genetics Consortium; International IBD Genetics Consortium. Association analyses identify 38 susceptibility loci for inflammatory bowel disease and highlight shared genetic risk across populations. Nat Genet 2015;47:979–986

25. Ellinghaus D, Jostins L, Spain SL, et al.; International IBD Genetics Consortium (IIBDGC); International Genetics of Ankylosing Spondylitis Consortium (IGAS); International PSC Study Group (IPSCSG); Genetic Analysis of Psoriasis Consortium (GAPC); Psoriasis Association Genetics Extension (PAGE). Analysis of five chronic inflammatory diseases identifies 27 new associations and highlights disease-specific patterns at shared loci. Nat Genet 2016;48:510–518

26. Swanson KD, Tang Y, Ceccarelli DF, et al. The Skap-hom dimerization and PH domains comprise a 3′-phosphoinositide-gated molecular switch. Mol Cell 2008;32:564–575

27. Pettersen EF, Goddard TD, Huang CC, et al. UCSF ChimeraX: structure visualization for researchers, educators, and developers. Protein Sci 2021;30:70–82

28. Langefeld CD, Ainsworth HC, Cunninghame Graham DS, et al. Transancestral mapping and genetic load in systemic lupus erythematosus. Nat Commun 2017;8:16021

29. Togni M, Swanson KD, Reimann S, et al. Regulation of in vitro and in vivo immune functions by the cytosolic adaptor protein SKAP-HOM. Mol Cell Biol 2005;25:8052–8063

30. Tsuchiya S, Yamabe M, Yamaguchi Y, Kobayashi Y, Konno T, Tada K. Establishment and characterization of a human acute monocytic leukemia cell line (THP-1). Int J Cancer 1980;26:171–176

31. Timms JF, Swanson KD, Marie-Cardine A, et al. SHPS-1 is a scaffold for assembling distinct adhesion-regulated multi-protein complexes in macrophages. Curr Biol 1999;9:927–930

32. Bompard G, Caron E. Regulation of WASP/WAVE proteins: making a long story short. J Cell Biol 2004;166:957–962

33. Deshmane SL, Kremlev S, Amini S, Sawaya BE. Monocyte chemoattractant protein-1 (MCP-1): an overview. J Interferon Cytokine Res 2009;29:313–326

34. Abram CL, Lowell CA. The ins and outs of leukocyte integrin signaling. Annu Rev Immunol 2009;27:339–362

35. Herter J, Zarbock A. Integrin regulation during leukocyte recruitment. J Immunol 2013;190:4451–4457

36. Mosser DM, Edwards JP. Exploring the full spectrum of macrophage activation. Nat Rev Immunol 2008;8:958–969

37. Herold KC, Vignali DA, Cooke A, Bluestone JA. Type 1 diabetes: translating mechanistic observations into effective clinical outcomes. Nat Rev Immunol 2013;13:243–256

38. Warshauer JT, Bluestone JA, Anderson MS. New frontiers in the treatment of type 1 diabetes. Cell Metab 2020;31:46–61

39. Carrero JA, McCarthy DP, Ferris ST, et al. Resident macrophages of pancreatic islets have a seminal role in the initiation of autoimmune diabetes of NOD mice. Proc Natl Acad Sci U S A 2017;114:E10418–E10427

40. Marro BS, Legrain S, Ware BC, Oldstone MB. Macrophage IFN-I signaling promotes

autoreactive T cell infiltration into islets in type 1 diabetes model. JCI Insight 2019;4: 125067
41. Zakharov PN, Hu H, Wan X, Unanue ER. Single-cell RNA sequencing of murine islets shows high cellular complexity at all stages of autoimmune diabetes. J Exp Med 2020;217:e20192362
42. Yin B, Ma G, Yen CY, et al. Myeloid-derived suppressor cells prevent type 1 diabetes in murine models. J Immunol 2010;185:5828–5834
43. Elizondo DM, Brandy NZ, da Silva RL, de Moura TR, Lipscomb MW. Allograft inflammatory factor-1 in myeloid cells drives autoimmunity in type 1 diabetes. JCI Insight 2020;5:136092
44. Campbell-Thompson M, Fu A, Kaddis JS, et al. Insulitis and β-cell mass in the natural history of type 1 diabetes. Diabetes 2016;65:719–731
45. Itoh N, Hanafusa T, Miyazaki A, et al. Mononuclear cell infiltration and its relation to the expression of major histocompatibility complex antigens and adhesion molecules in pancreas biopsy specimens from newly diagnosed insulin-dependent diabetes mellitus patients. J Clin Invest 1993;92:2313–2322
46. Abram CL, Roberge GL, Pao LI, Neel BG, Lowell CA. Distinct roles for neutrophils and dendritic cells in inflammation and autoimmunity in motheaten mice. Immunity 2013;38:489–501
47. Lamagna C, Scapini P, van Ziffle JA, DeFranco AL, Lowell CA. Hyperactivated MyD88 signaling in dendritic cells, through specific deletion of Lyn kinase, causes severe autoimmunity and inflammation. Proc Natl Acad Sci U S A 2013;110: E3311–E3320
48. Kool M, van Loo G, Waelput W, et al. The ubiquitin-editing protein A20 prevents dendritic cell activation, recognition of apoptotic cells, and systemic autoimmunity. Immunity 2011; 35:82–96